The cure reactions in the polyurethane matrix were studied by IR spectroscopy and also analyzed by second-order kinetic equations. Similar trends in the kinetic plot were also observed from IR monitoring of MDI, as were found from fluorescence monitoring of NDI. The second-order rate constants for MDI were found to be slightly greater than those for NDI at 50 and 70 °C. The activation energy of about 10 kcal/mol were estimated for both NDI and MDI. From these results, a calibration curve was established to correlate the extent of reaction for MDI with that for NDI. When the fluorescence results from polyurethane matrix were analyzed on the basis of two consecutive second-order reactions, the reactivity of the first isocyanate turned out to be similar to that of the second one in NDI.

Acknowledgment. We acknowledge the financial support of this work by the Army Research Office (Contract No. DAAG 29-85-K-0055 and DAAL03-87-G-0016) and National Science Foundation, Polymers Program (DMR 87-03908). We also extend our gratitude to P. Dickinson and A. Pirnia for constructive comments and help on the manuscript.

References and Notes

(1) Sung, C. S. P.; Pyun, E.; Sun, H.-L. *Macromolecules* **1986**, *19*, 2922.
(2) (a) Pyun, E.; Mathisen, R. J.; Sung, C. S. P. *Macromolecules* **1989**, *22*, 1174. (b) Dickinson, P.; Sung, C. S. P. *Polym. Prepr. (Am. Chem. Soc., Div. Polym. Chem.* **1988**, *29-1*, 530.
(3) Yoo, J. K.; Sung, C. S. P. *Polym. Mat. Sci. Eng.* **1989**, *60-1*, 429.
(4) Mathisen, R. J.; Yoo, J. K.; Sung, C. S. P. *Macromolecules* **1987**, *20*, 1414.
(5) Ferstandig, L. L.; Scherrer, L. L. *J. Am. Chem. Soc.* **1959**, *81*, 4838.
(6) Yu, W. C.; Huang, X. Y.; Sung, C. S. P. *Polym. Prepr. (Am. Chem. Soc., Div. Polym. Chem.)* **1988**, *29-1*, 532.
(7) Baker, J. W.; Holdsworth, J. B. *J. Chem. Soc.* **1947**, 713.
(8) Bailey, M. E.; Kirss, V.; Spaunburgh, R. G. *Ind. Eng. Chem.* **1956**, *8*, 794.
(9) Burkus, J.; Eckert, C. F. *J. Am. Chem. Soc.* **1958**, *80*, 5948.
(10) Barbalata, A. *Eur. Polym. J.* **1978**, *14*, 427.
(11) (a) Sato, M. *J. Am. Chem. Soc.* **1960**, *82*, 3893. (b) Greenshields, S. J. N.; Peters, R. H.; Stepto, R. F. T. *J. Chem. Soc.* **1964**, 5101.
(12) Dusek, K.; Bleha, M.; Lunak, S. *J. Polym. Sci., Polym. Chem. Ed.* **1977**, *15*, 2393.

Registry No. NDI, 3173-72-6; UI, 124244-57-1; DU, 124244-58-2; (MDI)(NDI)(PTMO) (copolymer), 124244-61-7; 1-butanol, 71-36-3.

Site-Selective Fluorescence Spectroscopy of Poly(vinylcarbazole)

U. Rauscher and H. Bässler*

Fachbereich Physikalische Chemie and Zentrum für Materialwissenschaften, Philipps-Universität, Hans-Meerwein-Strasse, D-3550 Marburg, FRG.
Received May 1, 1989

ABSTRACT: Site-selectively excited low-temperature fluorescence spectra are reported for matrix-isolated poly(styrene-*co*-vinylcarbazole) and poly(vinylcarbazole) in MTHF glass and for films of cationically and radically polymerized PVCA. The spectra of the copolymer indicate that isolated carbazole chromophores emit resonantly, the electron–phonon coupling constant being $S \leq 1$. Both in PVCA/MTHF and PVCA film excitations execute a random walk, as expected for an energetically disordered system, if initially generated above a localization energy ν_{loc} within the low-energy tail of the inhomogeneously broadened distribution of intrinsic CA states (ν_{loc} = 28.380 cm^{-1} for PVCA/MTHF and 27.700 cm^{-1} for PVCA film). In the glass emission comes from states at ν_{loc} while in PVCA films structural traps (excimer-forming sites and trap II sites) capture the excitations involving a combination of random walk and long-range Förster transfer. Upon exciting at $\nu_{ex} < \nu_{loc}$, defect states, showing up as a shoulder in the absorption and fluorescence excitation spectra of both PVCA/MTHF glasses and PVCA films, are populated directly, giving rise to fluorescence that shifts linearly with ν_{ex} and displays a Stokes shift of 800 and 1100 cm^{-1}, equivalent to an electron–phonon coupling constant $S = 3$. They are identified as the ground-state configurations of trap II.

1. Introduction

Poly(vinylcarbazole) (PVCA) can be considered as a prototype pendant group polymer whose electronic properties, for instance, the capability to transport charge carriers or optical excitations, are all controlled by the substituent rather than the main chain. In view of its principal importance for the photophysics and photochemistry of polymers, transfer of excitation (ET) has long been the subject of extensive work. It has meanwhile been established that PVCA does transport electronic excitation energy, albeit not quite as efficiently as molecular crystals do. Transport is envisaged as the random walk of excitations among the carbazole (CA) chromophores until trapping occurs at chemical or physical defects, although long-range Förster transfer may be involved in the ultimate capture process. (For a review see ref 1–3.)

Identification of ET is usually based on either steady-state luminescence experiments monitoring the fractional emission intensity of deliberately added guest molecules acting as energy sinks[4] or time-resolved studies of the decay of the host emission and buildup of a trap emission.[5–9] The traps can be of structural origin such as the strongly or weakly overlapping CA pairs in PVCA, giving rise to genuine excimer emission near 24 000 cm^{-1} and trap II emission near 26 600 cm^{-1}.[1,10–12] Although principally straightforward and well-tested on molecular crystals, these methods are often inconclusive if applied

0024-9297/90/2223-0398$02.50/0

to polymeric systems. A major problem is the width of the emission bands and their mutual overlap, which prevents monitoring the population kinetics of a selected molecular species in an unambiguous way. Moreover, determination of absolute transfer rates is complicated by the lack of a direct method for probing the concentration of structural traps and/or the difficulty of distinguishing whether it is the random walk of an excitation toward a deliberately added chemical trap or the ultimate capture process that limits the transfer rate.[13] Another concern, which so far has received limited attention only, is the role disorder plays for ET. Inhomogeneous broadening of absorption band profiles provides compelling evidence for the existence of energetic disorder ("diagonal" disorder) built into the structure. It results from the statistics of the van der Waals interaction energy of a chromophore with an environment subject to positional disorder as realized in a random solid.[14-16] This effect is irrelevant at temperatures where the standard deviation of the disorder potential (σ) is of order kT yet ought to gain importance at low T, because excitations tend to settle to the tail states of the distribution. In fluid polymer solutions the situation is even more complex because of the rapid molecular motion causing temporal fluctuation of the local transfer rates. Nonexponential decay of the monomer emission and buildup of excimer emission in PVCA solutions are then a reflection of dynamic disorder, albeit difficult to deconvolute.[17]

The aim of the present study is to demonstrate that the technique of steady-state site-selective laser spectroscopy[18] can profitably be applied to PVCA for elucidating and separating homogeneous and inhomogeneous line-broadening mechanisms and for probing excitation transport. The advantage of this method is that it does not rely on extrinsic probe molecules but uses a subset of chromophores in resonance with the exciting laser as a probe for excitation dynamics. It will be shown that the loss of site memory an excitation suffers after being generated at a given energy with the inhomogeneous absorption profile provides a handle on problems like (i) the origin of the Stokes shift, (ii) the strength of electron–phonon coupling, (iii) the dimensionality of the random walk of an excitation, (iv) excitation localization, and (v) the energetic distribution of physical traps in PVCA. To aid separation of photophysical intrachromophore processes from interchromophore processes, a series of systems has been investigated exhibiting increasing strength of interchromophore interaction: (i) a dilute glass of a styrene/vinylcarbazole copolymer with low carbazole (CA) content, (ii) a dilute PVCA/2-methyltetrahydrofuran (MTHF) glass, and (iii) solid films of cationically and radically polymerized PVCA films.

2. Analysis of Site-Selective Fluorescence (SSF) Spectra

Before experimental results are presented, it appears appropriate to outline the concept of analyzing fluorescence spectra recorded upon site-selective excitation. Consider an ensemble of absorbers whose electronic origins are subject to an inhomogeneous distribution $g(\nu_0)$, usually adequately described by a Gaussian distribution function centered at ν_m[16,19]

$$g(\nu_0) = (2\pi\sigma^2)^{-1/2} \exp[-(\nu_0 - \nu_m)^2/2\sigma^2] \quad (1)$$

Each individual absorber is characterized by the homogeneous spectral distribution functions $\epsilon(\nu' - \nu_0)$ and $\phi(\nu - \nu_0)$ for absorption and emission, respectively. Equation 1 represents the experimentally observed absorption spectrum in the case that the homogeneous line widths are $\ll\sigma$. The SSF spectrum of the vibronic 0–0 transition recorded upon exciting with a δ-shaped laser line at ν_{ex} is the convolution of $g(\nu_0)$ and the homogeneous line-shape functions

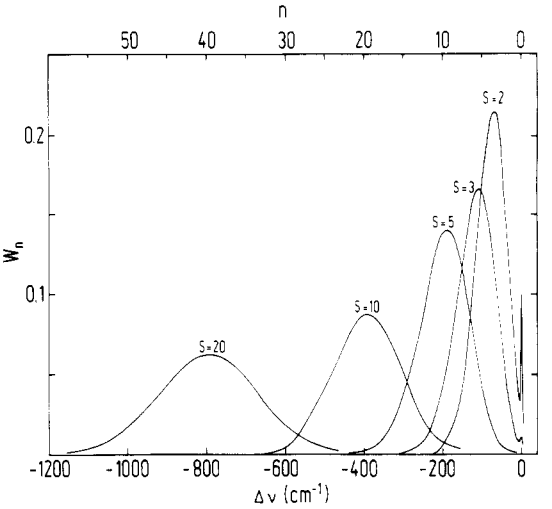

Figure 1. Fluorescence profiles calculated on the basis of eq 3 parametric in S assuming linear electron–phonon coupling. n is the number of phonons involved in a transition. The abscissa scale has been drawn for a phonon frequency $\hbar w_{ph} = 20$ cm^{-1}.

$$F(\nu,\nu_{ex}) = \int_0^\infty \phi(\nu - \nu_0)\, \epsilon(\nu_{ex} - \nu_0)\, g(\nu_0)\, d\nu_0 \quad (2)$$

If $g(\nu_0)$ is a smoothly varying function compared to $\epsilon(\nu' - \nu_0)$ and $\phi(\nu - \nu_0)$, eq 2 reduces to

$$F(\nu,\nu_{ex}) \propto \int_0^\infty \phi(\nu - \nu_0)\, \epsilon(\nu_{ex} - \nu_0)\, d\nu_0 \quad (3)$$

In the same approximation the fluorescence excitation spectrum recorded at a fixed emission energy, ν_{em}, is

$$FE(\nu', \nu_{em}) = \int_0^\infty \phi(\nu_{em} - \nu_0)\, \epsilon(\nu' - \nu_0)\, d\nu_0 \quad (4)$$

Equations 3 and 4 are easily generalized for arbitrary vibronic transitions.

At low temperatures the homogeneous line-shape functions consist of a zero phonon (ZP) line followed by a phonon wing (PW). The fractional ZP intensity

$$I_{ZP}/I_{total} = \alpha = e^{-S} \quad (5)$$

is called the Debye–Weller factor reflecting the strength of the electron–phonon expressed in terms of the Huang–Rhys factor S. In case of a single phonon mode of energy $\hbar w_{ph}$, the intensity distribution in the PW follows a Poisson distribution

$$W_n = S_v^n e^{-S_v}/n! \quad (6)$$

where n is the number of phonons involved and v specifies the vibrational quantum state of the chromophore. In view of both the rich optical phonon spectrum of organic solids and inhomogeneous broadening in random media, phonon wings if chromophores in low-temperature glasses are rather structureless.[19,20]

As a guideline for analyzing experimental SSF spectra, a series of PW profiles is presented in Figure 1 calculated on the basis of eq 3 assuming (i) Poisson distributions for the PWs of the homogeneous absorption and emission profiles and (ii) linear electron–phonon coupling, i.e., the same curvature of the energy parabolas in ground and excited state equivalent to constant phonon

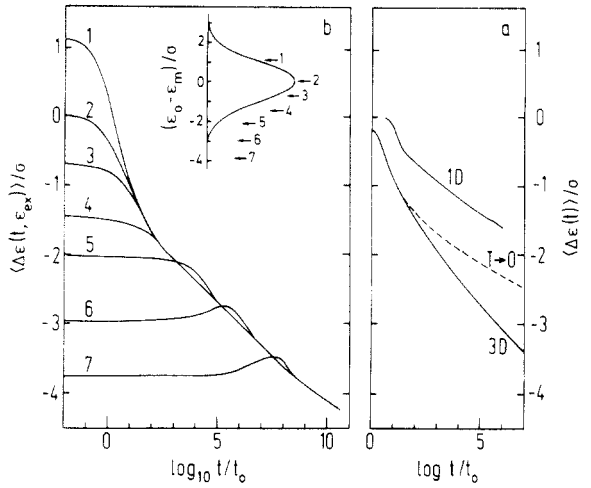

Figure 2. Temporal decay of the mean energy of an ensemble of noninteracting excitations executing a random walk within a Gaussian distribution of hopping states. σ is the Gaussian width of the DOS. (a) Simulation results for random initial population of a three-dimensional and one-dimensional array of hopping sites, respectively, characterized by a disorder parameter $\sigma/kT = 4.5$. The dashed curve represents the 3D and $T \rightarrow 0$ case. (b) Simulation and analytic results for site-selective initial population at the indicated energetic positions within the DOS for $\sigma/kT = 4.5$ (adapted after ref 22).

energy. Even for $S = 2$, which represents a case of moderate electron–phonon coupling, ZP lines are very weak already. With increasing S, the Stokes shift, δ, defined as the displacement of the PW maximum from the laser line, varies as $\delta = 2S\hbar w_{ph}$ and the PW envelope approaches a Gaussian of Gaussian width $\sigma_{PW} = \hbar w_{ph}(2S)^{1/2}$, i.e.

$$\sigma_{PW}/\delta = (2S)^{-1/2} \tag{7}$$

For more detailed discussion the reader is referred to the article by Personov.[18]

The above treatment is restricted to an array of chromophores sufficiently dilute to exclude interaction. Otherwise energy transfer will occur leading to spectral diffusion and a concomitant erosion if site memory. The framework for rationalizing the diffusion of excitations in random phases with static energetic disorder of the hopping sites has recently been developed.[21,22] Its basic elements shall briefly be recalled. Consider a one-component glass whose constituents establish a Gaussian distribution of electronic excitation energies of width σ. (Throughout this article Gaussian widths, i.e., standard deviations, will be used to quantify the widths of distributions of states (DOS) or of spectral bands.) An excitation initially generated at random is subject to a random walk in the course of which it will relax energetically toward the tail states of the distribution thereby slowing down its motion. At intermediate temperatures characterized by $\sigma/kT \lesssim 5$, the mean energy of a packet of independent excitations decays approximately logarithmically with time to finally settle at a mean energy $-\sigma^2/kT$ below the center of the DOS. At very low T where intervening temperature-activated jumps are eliminated, relaxation is slowed down approaching a (ln ln t)$^{1/2}$ law in the long time limit.[23] In a one-dimensional array of hopping sites relaxation is retarded as compared to the 3D case. Figure 2a portrays the results of Monte Carlo computer simulations for excitations migrating via exchange interaction. Their equivalence with analytic results has been demonstrated before[22,23] as well as the applicability of the concept to systems where excitation transport occurs via dipole coupling. Non-site-

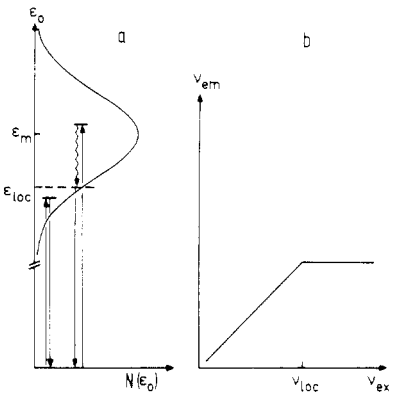

Figure 3. (a) Schematic view of nonresonant and resonant emission upon excitation at $\epsilon_{ex} > \epsilon_{loc}$ and $\epsilon_{ex} < \epsilon_{loc}$, respectively. (b) Schematic dependence of the mean emission energy ν_{ex} on excitation energy ν_{em}. (Here energies are denoted by ν.)

selective spectral diffusion experiments probing triplet excitation transport in glassy benzophenone[24,25] support the model.

The fact that the jump rate of an excitation depends on is energetic position within the distribution of excitation energies implies site selectivity of excitation transfer. Excitations generated at a well-defined energy within the DOS rather than statistically will become subject to subsequent diffusion and relaxation not until a waiting time has elapsed determined by the site-specific dwell time of an excitation (see Figure 2b). If it exceeds the intrinsic lifetime of the excitation, the excitation will be localized for its entire life. Scanning an exciting laser across the inhomogeneously broadened absorption profile of a glass will, therefore, reveal a localization phenomenon at a critical excitation energy, ν_{loc}. (Spectral energies will be given in wavenumber units.) For $\nu_{ex} > \nu_{loc}$ excitations are subject to relaxation and accumulate in states near ν_{loc} where they decay radiatively or nonradiatively, independent of ν_{ex}. The stochastic character of the random walk implies spectral diffusion, the width of the final distribution of occupied states becoming comparable to the width of the distribution of excitation energies.[26] For $\nu_{ex} < \nu_{loc}$, emission originates from the initially excited sites. The emission energy must, therefore, scale linearly with ν_{ex}, and emission spectra must be line-narrowed. A schematic view of the ν_{em}–ν_{ex} relation is depicted in Figure 3. Experimental evidence for this behavior has been derived from SSF spectra of glassy solutions of polydiacetylenes where excitation transport occurs along the configurationally disordered conjugated backbone.[27] Vanishing of singlet excitation transport to chemical traps in a 9,10-diphenylanthracene glass upon scanning the laser across the inhomogeneously broadened DOS has also been reported.[28]

3. Experimental Section

Site-selective fluorescence (SSF) as well as fluorescence excitation (SSFE) spectra were recorded upon excitation with an excimer laser pumped tunable dye laser system (Lambda-Physik) of spectral bandwidth 0.15 ± 0.05 cm^{-1}. Fluorescence was spectrally resolved by a Jobin Yvon U1000 double monochromator and recorded by a cooled Hamamatsu photomultiplier in conjunction with a Boxcar signal averager. To record the excitation spectrum of a particular emission band, the monochromator was scanned simultaneously with the exciting laser, thus maintaining a constant energy difference between excitation and detection. Samples, consisting of a frozen solution of the polymer in MTHF contained in a 2-mm quartz cuvette or a PVCA film deposited onto a quartz substrate, respectively, were attached to the cold finger of either a commercial or a

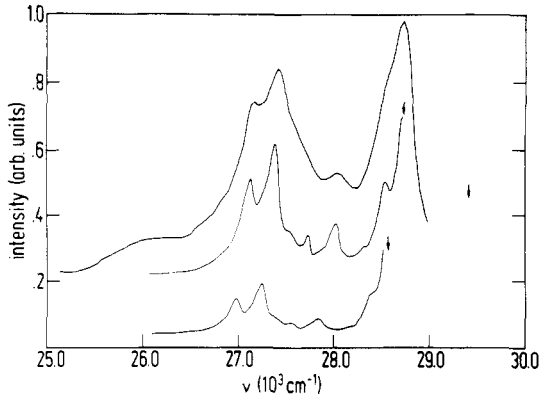

Figure 4. Site-selective fluorescence spectra of poly(styrene-*co*-vinylcarbazole) in MTHF glass at 15 K. Excitation energies are indicated by arrows.

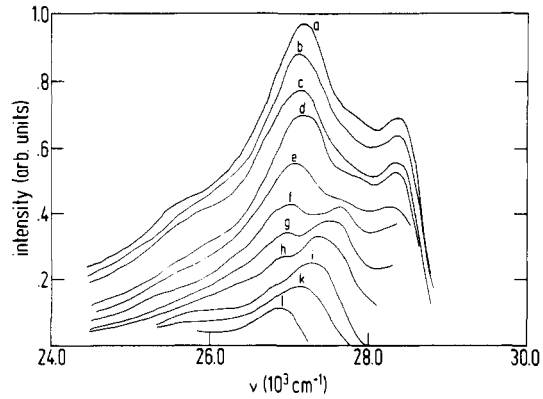

Figure 5. SSF spectra of cationic PVCA in MTHF glass (T = 15 K), parametric in the excitation energy ν_{ex}. Spectra are corrected for instrumental response; ordinate scales are arbitrary. Excitation energies (in cm^{-1}) were the following: a, 29.411; b, 29.239; c, 29.069; d, 28.653; e, 28.571; f, 28.409; g, 28.328; h, 28.248; i, 28.089; k, 27.932; l, 27.624.

home-built He-flow cryostat, yielding sample temperatures of 4.5 and $\simeq$15 K, respectively.

Cationically and radically polymerized PVCA of molecular weight (3–5) $\times 10^6$ was kindly placed to our disposal by Professor W. Klöpffer. Low molecular weight impurities, such as anthracene, were removed by 3-fold precipitation from benzene solution with methanol and subsequent gel permeation chromatography using Merckogel OR 6000. Poly(styrene-*co*-vinylcarbazole) was synthesized by radical polymerization in solution containing the monomers in a 50:1 molar ratio.

4. Results

A series of 15 KSSF spectra of the CA/styrene copolymer parametric in excitation energy ν_{ex} are presented in Figure 4. As long as ν_{ex} is close to the peak energy of the inhomogeneously broadened $S_1 \leftarrow S_0$ 0–0 absorption profile, known to be located near 28 900 cm^{-1} for glassy solutions of monomeric *N*-methylcarbazole,[29] a dimeric model compound [1,3-bis(carbazolylpropane)[3]], and PVCA in both solid solution and solid film,[3,30] emission spectra are independent of ν_{ex}. They extrapolate to an electronic origin near 28 800 cm^{-1} and reveal some inhomogeneous broadening. Line-narrowed fluorescence spectra, resonant with the laser, have been observed for ν_{ex} < 28 800 cm^{-1}. Absence of a sharp zero phonon feature can be attributed to temperature broadening. Not only do the spectra allow determination of the dominant vibrational frequencies (685, 1305, and 1578 cm^{-1}) but they also document that the SSF spectrum of an electronically decoupled CA group attached to a vinyl polymer chain is the same as that of a monomeric chromophore dispersed in a glassy matrix. The electron–phonon coupling constant S must be of order unity or less, comparable to what has been found for monomeric emitters dispersed in a polymer matrix.[31,32] Deviation from resonance upon exciting at ν_{ex} > 28 800 cm^{-1} is readily attributed to the onset of energy transfer accompanied by some spectral diffusion. The shift of the localization threshold ν_{loc} toward the center of the absorption profile as compared to PVCA (see below) reflects the dilution of transport states in the copolymer.

SSF spectra of PVCA in glassy MTHF solution are devoid of sharp features at all excitation energies (Figure 5). For ν_{ex} > 28 400 cm^{-1} the spectrum is characteristic of a common monomeric emitting state. The peak of the inhomogeneously broadened $S_1 \rightarrow S_0$ 0–0 transition occurs at 28 380 ± 20 cm^{-1}, independent of ν_{ex}. It is followed by a broad vibronic band assigned to the superposition of the 1305- and 1578-cm^{-1} modes. The high-energy tail of the 0–0 emission band is of Gaussian shape of (Gaussian) width 270 cm^{-1}, comparable to the width

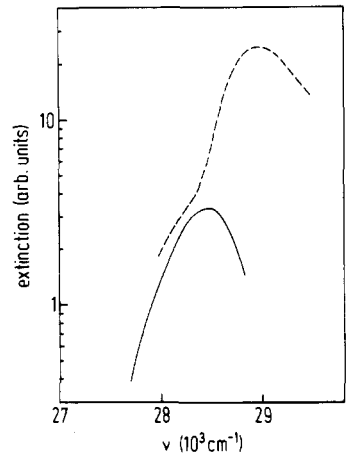

Figure 6. Comparison between the defect fluorescence excitation spectrum of matrix-isolated PVCA, recorded upon keeping the energy difference between ν_{ex} and ν_{em} fixed, and the total absorption spectrum of the glass taken from ref 3.

of the $S_1 \leftarrow S_0$ 0–0 absorption band in glassy matrix (see Figure 6). When ν_{ex} is decreased beyond 28 500 cm^{-1}, a broad emission feature appears that shifts linearly with ν_{ex}, its peaks being offset by 800 cm^{-1} from the laser. An analysis of this behavior in terms of a ν_{em}–ν_{ex} relation is presented in Figure 7. The excitation spectrum of the additional band, recorded upon maintaining a constant energy separation of 720 cm^{-1} between excitation and detection, is a broad band with an approximately Gaussian tail with standard deviation 320 cm^{-1} (Figure 6). It obviously corresponds to the shoulder seen in the tail of the absorption spectrum, which must be the signature of a defect state, whatever its relation to structural defects giving rise to weakly or strongly bound excimer emission may be.

The difference between SSF spectra of PVCA in glassy solution and in solid film, respectively, is the replacement of the monomer emission by trap II emission, peaking at 26 600 cm^{-1}, and the excimer band near 24 000 cm^{-1}, the latter being more pronounced in cationically polymerized samples (Figures 8 and 9). A weak high-energy shoulder indicates that a small fraction of monomer excitations escapes trapping by defects. It increases with decreasing ν_{ex} as is expected on the basis of energy-dependent excitation transfer. As ν_{ex} decreases an additional feature appears at the high-energy shoulder of trap II emission that shifts linearly with ν_{ex} (Figure 10). It is

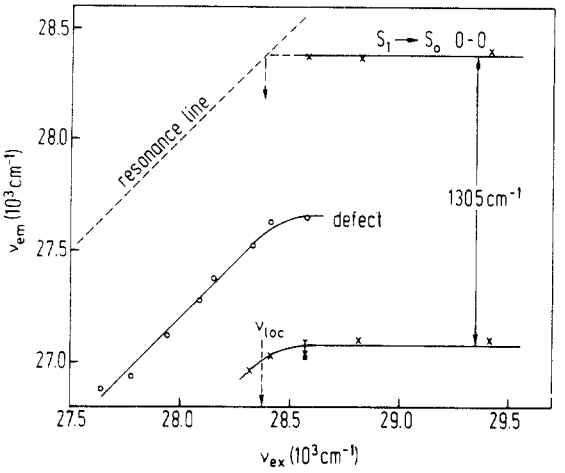

Figure 7. Peak energies ν_{em} of the fluorescence bands of PVCA in MTHF glass taken from Figure 5 and plotted as a function of excitation energy ν_{ex}. Crosses refer to the $S_1 \rightarrow S_0$ 0–0 and 0–1 transitions of the relaxed monomer, circles refer to the defect (trap II).

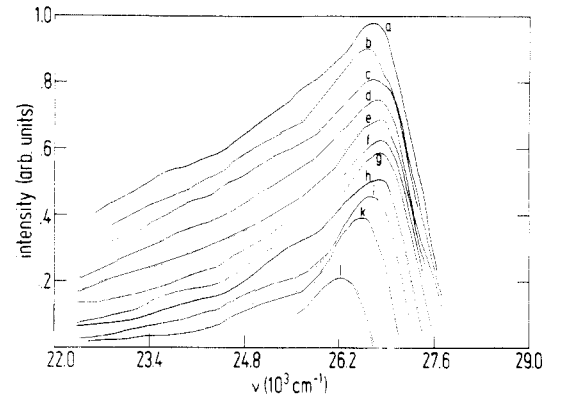

Figure 8. SSF spectra of cationicaly polymerized PVCA films parametric in ν_{ex}. Spectra have been corrected for instrumental response; ordinate scales are arbitrary. Excitation energies (in cm^{-1}) were the following: a, 29.239; b, 29.069; c, 28.735; d, 28.571; e, 28.409; f, 28.248; g, 28.089; h, 27.932; i, 27.777; k, 27.624; l, 27.322.

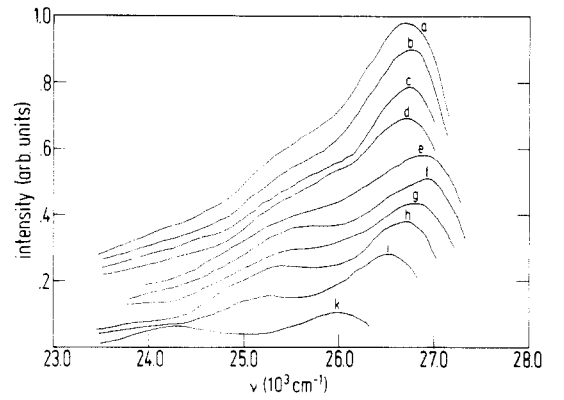

Figure 9. SSF spectra of radically polymerized PVCA films parametric in ν_{ex}. Excitation energies (in cm^{-1}) were the following: a, 29.411; b, 29.239; c, 29.069; d, 28.985; e, 28.248; f, 28.089; g, 27.932; h, 27.777; i, 27.624; k, 27.173.

complementary to the defect band seen in the PVCA/MTHF spectra and is obviously due to direct excitation of defect states showing up as a shoulder in the film absorption spectrum (Figure 11).

Remarkably, monitoring the intensity of the excimer emission at 24 000 cm^{-1} as a function of ν_{ex} yields an excitation spectrum with a low-energy tail that parallels the tail of the defect band mentioned above (see Figure 11).

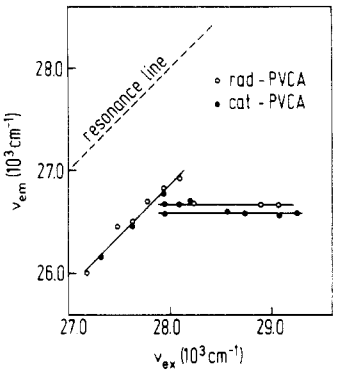

Figure 10. Peak energies ν_{em} of PVCA film fluorescence bands, taken from Figures 8 and 9 as a function of ν_{ex}. The horizontal straight lines correspond to trap II emission populated via energy transfer; open and closed circles refer to directly excited trap II emission.

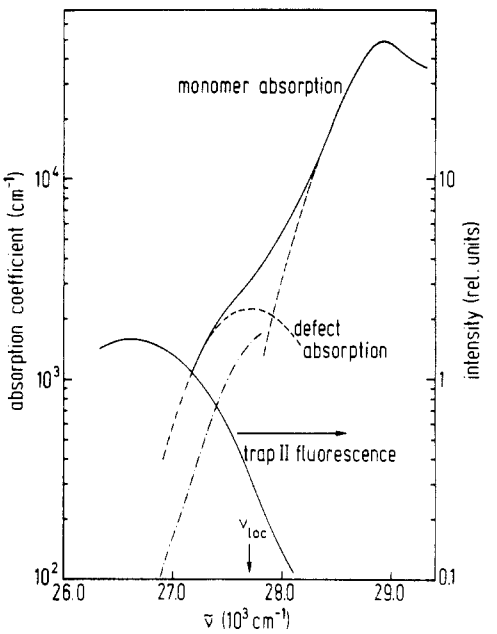

Figure 11. Absorption spectrum of a cationic PVCA film revealing the monomer and defect absorption peaks (after ref 30). The dash-dotted curve is the low-energy tail of the excitation spectrum for the excimer emission monitored at 24 000 cm^{-1} (the vertical position is arbitrary). Also shown is the trap II emission spectrum upon exciting at 29 240 cm^{-1}.

Since at those excitation energies energy transport is excluded, this observation demonstrates that the configuration giving rise to excimer emission has an optically allowed tansition red-shifted relative to the monomer peak.

5. Discussion

5.1. SSF Spectroscopy of Matrix-Isolated PVCA. The site-selectively recorded fluorescence spectra of PVCA in a glassy MTHF matrix represent an unambiguous example for the occurrence of excitation localization within an energetically disordered incoherent energy transport system and the concomitant turnover from inhomogeneous to essentially homogeneous line broadening in conjunction with the appearance of a Stokes shift. When we recall the message of Figure 4 that the emission spectrum of an electronically decoupled CA chromophore of the styrene/CA copolymer is resonant with the laser suggestive of weak electron–phonon coupling ($S \lesssim 1$), both the line broadening of the monomer $S_1 \rightarrow S_0$ 0–0 transition as well as its independence of ν_{ex} is a stringent test

on the occurrence of a random walk of an excitation among the CA chromophores. In its course spectral diffusion occurs. The high-energy tail of the emission spectrum has a width comparable to that of the inhomogeneously broadened intrinsic $S_1 \leftarrow S_0$ 0–0 absorption band as predicted by the model. It decreases somewhat as ν_{ex} is lowered. This is in accord with the notion that excitation transport should become less efficient as ν_{ex} approaches ν_{loc}. The emission peak monitors the average energy of the populated states within the DOS. Intersection of the extrapolated $\nu_{em}-\nu_{ex}$ line with the resonance line in Figure 6 yields a localization energy $\nu_{loc} = 28\,380$ cm^{-1}.

The ratio of the mean energy loss $\Delta\nu = \nu_m - \nu_{loc}$ due to excitation relaxation to the width σ of the DOS is $\Delta\nu/\sigma \simeq 520$ cm^{-1}/300 cm$^{-1} \simeq 1.8$. For PVCA in a 77 K toluene glass the monomer emission peak is at 28 100 cm^{-1},[3] yielding $\Delta\nu = 800$ cm^{-1} and $\Delta\nu/\sigma \simeq 2.5$. The increase of $\Delta\nu$ at 77 K, as compared to 15 K, is in accord with theory predicting that thermal activation aids an excitation to find additional pathways for subsequent relaxation.[21,22] Comparison of $\Delta\nu/\sigma$ values with the simulation data of Figure 2a allows arguing on the dimensionality of the random walk. Taking 5 ns as a representative value for the lifetime of a CA singlet state—values ranging from 4 to 7 ns have been measured for the short luminescence component[9,33]—and assuming $t_0 = 10^{13}$ s as a lower bound for the excitation jump time among adjacent CA groups predicts $\Delta\nu/\sigma \leq 2.5$ and ≤ 2.0 for $T = 77$ and 9 K, respectively, in the case of 3D random walk and $\Delta\nu/\sigma \leq 1.1$ for 1D topology at 77 K. The experimental data would seem to favor the 3D case, contrary to the conclusions Fitzgibbon and Frank draw from the molecular weight dependence of excimer formation in matrix-isolated poly vinylnaphthalene).[34] A cautionary note is, however, in order, because the assumption of exchange interaction, underlying the simulations, may lead to an underestimation of energy relaxation in the 1D system where non-nearest-neighbor interactions are crucial.

The appearance of an additional emission band in the PVCA/MTHF spectrum shifting linearly with ν_{ex} upon exciting at $\nu_{ex} < 28\,500$ cm^{-1} indicates participation of an emitting state different from the monomer. It can be populated either directly or via ET from monomer states. If the excitation spectrum of this emission is recorded under preservation of a fixed energy separation between excitation and emission, as was done to collect the data of Figure 6, direct excitation prevails and the corresponding FE spectrum reflects the true defect absorption spectrum. It peaks at 28 450 cm^{-1}, about 450 cm^{-1} below the center of the monomer absorption band, its Gaussian widths (320 cm^{-1}) being comparable to that of the intrinsic monomer absorption band. The defect emission spectrum, monitored upon exciting at $\nu_{ex} \leq 28\,200$ cm^{-1}, where both ET to the defect is absent and absorption by monomer states is negligible, is characteristic of an emitter with intermediate electron–phonon coupling strength. On the basis of a Stokes shift $\delta = 800$ cm^{-1} and a width of the high-energy tail $\sigma_{PW} = 330$ cm^{-1}, $S = 3$, is calculated applying eq 7. Since $\delta = 2S\hbar w_{ph}$, $\hbar w_{ph} = 130$ cm^{-1} is obtained for the energy of the dominant phonon mode. It is close to the energy estimated for the mutual vibration of a pair of incipient pyrene molecules in a pyrene crystal.[35] The facts that (i) this defect is not found in the copolymer and (ii) the S value is larger than that for a monomeric CA chromophore suggest associating the defect with the CA pair structure. On the basis of PVCA film spectra, it will be identified as trap II.

If excitations occur above ν_{loc} the pair emission can be sensitized by energy transfer from monomer states as well as indicated by the shoulder in the fluorescence spectrum near 27 650 cm^{-1}. (Note that resonant FE detection, as has been applied to collect the spectrum in Figure 6, precludes detecting nonresonant population channels.) In this case the pair emission spectrum is the image of the inhomogeneously broadened pair absorption spectrum, red-shifted by the Stokes shift of 800 cm^{-1}.

5.2. SSF Spectroscopy of PVCA Films. On the basis of the scenario developed for rationalizing SSF spectra of matrix-isolated PVCA, the spectra of PVCA films can be interpreted in a consistent manner if one invokes an increase of the rate of excitation trapping by structural traps. Absorption spectroscopy indicates that the main differences between dilute glass and solid film are (i) an increase of the Gaussian widths of the inhomogeneous absorption profiles of both CA monomer and defect to $\simeq$500 cm^{-1} and (ii) an increase of the displacement of the defect band relative to the monomer band to 1200 cm^{-1} (Figure 11). The relative height of the defect band remains unchanged. SSF spectra recorded upon exciting at energies where the defect is selectively populated indicate a linear shift of the defect emission with ν_{ex}, its peak being offset from the laser by $\delta = 1100$ cm^{-1} (Figure 10). At the same time the width σ_{PW} of the high-energy tail of the defect 0–0 emission has increased to 440 cm^{-1}, thus maintaining the ratio $\sigma_{PW}/\delta = 0.4$, equivalent to an electron–phonon coupling constant $S = 3$, unaltered relative to the glass. Only the energy of the phonon frequency has increased to 180 cm^{-1}. This is readily explained in terms of the more rigid environment of a weakly bound pair of CA units sitting in a PVCA film as compared to a glass. The high-energy part of the emission spectra of a cationic PVCA film can be reproduced in a satisfactory manner by the superposition of electronic and vibronic transitions involving the 685- and 1305-cm^{-1} intramolecular modes, each being subject to coupling to an intramolecular mode assuming $S = 3$.

Knowing that the maximum of the defect absorption band in the PVCA film is at 27 700 cm^{-1} and the Stokes shift due to pair relaxation is 1100 cm^{-1}, one would locate the maximum of the inhomogeneously broadened defect emission band at 26 600 cm^{-1}. The fact that trap II emission peaks at exactly that energy is another test in favor of assigning this defect to the pair of weakly overlapping CA groups giving rise to trap II emission. Both the short fluorescence lifetime of the pair and the observation of finite oscillator strength in absorption require that the transition moments of the participant CA groups be nonparallel. The molecular planes must, however, be close to parallelity in order to facilitate pair relaxation after excitation and to account for the red-shift of the absorption spectrum relative to a CA bulk chromophore. We are aware that identifying the defect absorption band with a pair of CA molecules acting as precursor of trap II emission is at variance with earlier estimates of the concentration of trap II configurations. On the basis of an analysis of the energy-transfer efficiency, Rippen et al.[12] estimate the relative trap II concentration to be of order $c_{II} \simeq 10^{-3}$ per monomer unit while the ratio of the peak absorbances of monomer CA and defect (Figures 6 and 11) suggest that c_{II} be at least 1 order of magnitude larger. We shall return to this problem in section 5.3.

With the above results in mind, SSF spectra recorded upon scanning the excitation laser across the absorption profile of a PVCA film can be explained in a straightforward manner. As long as ν_{ex} is above ν_{loc}, excitations execute a random walk within the monomer DOS. In its course they are trapped at either weakly or strongly over-

lapping CA pairs and populate the distribution of pair states statistically. Defect emission is therefore independent of ν_{ex} and reflects the inhomogeneously broadened pair fluorescence spectrum. As ν_{ex} reaches 28 000 cm^{-1} where in the film defect absorption begins to dominate, site-selective trap II emission shows up at the high-energy tail of the inhomogeneously broadened trap II emission. It grows at the expense of the latter, which decreases because ET is gradually eliminated as ν_{ex} approaches ν_{loc}. Note that, once excited, the trap II state can no longer transfer energy because of rapid intrapair relaxation. Unfortunately, the absence of monomer emission precludes direct determination of the localization threshold ν_{loc}. A rough estimate can, however, be obtained from the disappearance for the 26 600-cm^{-1} band, known to be due to indirectly populated trap II states. For radical PVCA this occurs between 27 780 and 27 620 cm^{-1}. Taking $\nu_{loc} \simeq 27.700$ cm^{-1} as an average value yields $\Delta\nu/\sigma \simeq 2.4$ for the excitation relaxation energy at 15 K normalized to the DOS bandwidth. It is somewhat larger than the value obtained for matrix-isolated PVCA (see above). Not only is this a verification of the expected 3D character of excitation transport in solid films of PVCA but it also demonstrates that excitation transport is more efficient in the film than in a matrix-isolated molecule because an excitation sitting on a CA chromophore in a film has more options for jumping to adjacent acceptors. As a consequence, excitations can relax to deeper states of the monomer DOS.

5.3. Remarks on the Efficiency of Excitation Transport in PVCA Films. Observation of site-selective energy transfer in matrix-isolated PVCA and PVCA solid film is an unambiguous signature of the random-walk excitations performance within the manifold of intrinsic singlet states. In its course either sandwich pair or trap II configurations are populated resulting in sensitized trap emission. However, attempts to rationalize low temperatures and site-selective excitation transfer in PVCA in terms of the random-walk concept alone lead to an inconsistency. Recall that the probability of an excitation to reach a trap, present at relative concentration c, after having executed n jumps[36] is

$$P_t = 1 - (1 - c)^n \tag{8}$$

For $n_c \ll 1$, $P_t \approx nc$ yielding a ratio of trap to host emission

$$I_t/I_h = P_t/(1 - P_t) \tag{9}$$

if quantum efficiencies of trap and host luminescence are assumed equal. In case of two competing types of traps, present in relative concentrations c_I and c_{II}, the total trap emission is still given by eq 9, while the fractional trap emission intensities are

$$I_{t_I}/I_{t_{II}} = c_I/c_{II} \tag{10}$$

independent of the diffusivity of the excitation expressed in terms of n.

From the reduction of excimer fluorescence of PVCA upon addition of chemical traps the concentration of excimer sites has been estimated to be $c_I \approx 2 \times 10^{-3}$. Ignoring tacticity-dependent variations, the concentration of trap II sites has been assumed to be of the same order of magnitude. Adopting the value $k_h = 2 \times 10^{12}$ s^{-1} for S_1 transport,[37] $n = k_h\tau_f \approx 10^4$ follows assuming a monomer fluorescence lifetime of 5 ns. Hence, $P_t \simeq 1$, in accord with the complete absence of monomer emission at 300 K.

The following observations are, however, at variance with this simple concept.

(i) Upon reduction of excitation diffusion by lowering the temperature trap II, emission increases at the expense of the excimer band, contrary to eq 10 predicting a branching ratio that remains constant.

(ii) Both earlier site-selective ET studies at 77 K[30] and the present 15 K data (Figures 8 and 9) indicate that the efficiency of excitation transport toward excimer-forming sites is reduced upon decreasing ν_{ex}. If combined with statement (i), one has to conclude that excimer-forming sites are populated less efficiently as the diffusivity of the excitations decreases.

(iii) Monte Carlo computer simulations, carried out after completing the work reported in ref 30, yielded the number of new sites an excitation visits within its lifetime as a function of the disorder parameter σ/kT.[38] For $\sigma/kT = 2.5$, characteristic of a PVCA film at 300 K ($\sigma = 500$ cm^{-1}), excitation diffusion becomes time-independent within the S_1 lifetime and the number of jumps (n) is estimated to be about 1 order of magnitude less than in a crystalline counterpart system, yet still sufficiently large to yield $P_t \simeq 1$ (eq 8). However, for $T = 77$ and 15 K, corresponding to $\sigma/kT \approx 10$ and 50, respectively, n is reduced to values of order 10 or even less! Admittedly, those computations were performed for the case of exchange interaction. However, in the case of the farther reaching dipole coupling n could only be less since energy relaxation per jump could only increase. Equation 8 would then predict that only about 2% of all excitations become trapped, in striking disagreement with experiment. The simulations, well tested by independent experiments,[24,25] thus demonstrate that at low T the excitations have relaxed to states where further diffusive transport is blocked, long before their majority has reached a trap.

The discrepancy between the predictions of random-walk theory and low-T trapping experiments thus call for invoking a combination of dispersive multistep excitation transport and long-range Förster transport. Unfortunately, the neglect of energy relaxation prevents direct application of the pertinent analytic treatment of Gösele et al.[39] to PVCA at low T. Qualitatively, the following scenario can be envisaged. Excitation transport toward an energy sink always follows the fastest route. At 300 K transport is diffusive and long-range transport is unimportant. Long-distance single-step transfer will take over if the velocity of the random walk becomes prohibitively slow. If both transfer modes coexist, the random walk allows an excitation surveying its neighborhood for favorable subsequent long-range transfer steps. Consider a random PVCA structure containing the two types of traps present in concentration c_I and c_{II}, respectively. At temperatures sufficiently high to ensure that kT is comparable to the width of the DOS, excitation transport is diffusion-controlled and populates the low-energy trap preferentially because trap II can be emptied thermally. At low T long-range transfer aided by diffusion becomes important. Depending on the ratio of the diffusion length to the mean distance an excitation has to overcome in order to get trapped, the latter effect favors population of the trap present in higher concentration. This explains why (i) at low T/low ν_{ex} trap II emission dominates and (ii) the total trap emission is larger than predicted by eq 8 provided that two conditions are met: (1) c_{II} must exceed c_I. This is in accord with the absorbance of the tail states in PVCA films (Figure 11) yet at variance with literature results.[12] However, those estimates have been derived

from energy-transfer studies and may, by virtue of the arguments presented in this work, be subject to considerable uncertainty. (2) Spectral overlap between the monomer states near ν_{loc} and both types of traps must be sufficiently large. This is at variance with the widely accepted, yet unproven, notion that the ground state of the trap giving rise to excimer emission is a sandwich pair of CA chromophores having a parity forbidden low-energy transition. The excimer excitation spectrum shown in Figure 11 strongly argues against this view and confirms that the molecular axes of the CA chromophores forming the ground state of the excimer site must be tilted.

Additional support for the convolution of Förster-type transfer and dispersive energy migration controlling population of the excimer-forming sites in PVCA films comes from time-resolved studies monitoring buildup of the excimer emission at low T. They indicated a $t^{-(1-\alpha)}$ law for the population rate with $\alpha \simeq 0.2$ for $T \leq 40$ K while in the case of a pure random walk one would expect a dispersion parameter $\alpha = 0$ in the $T \rightarrow 0$ limit. This has been verified by energy-transfer studies in orientationally disordered 2,3-dimethylnaphthalene crystals[40] as well as geminate pair recombination studies in PVCA.[41] On the other hand, pure Förster-type transfer leads to a time dependence of the trapping rate of the form $k_t \sim t^{-0.5}$.[42]

6. Conclusions

It has been shown that site-selective low-temperature fluorescence spectroscopy can be employed to distinguish between excitation relaxation in the course of their random walk and structural relaxation as the possible origins of the Stokes shift seen in the emission spectra of PVCA. The random walk of the excitation has consistently been analyzed in terms of the concept of diffusion and relaxation of excitations within an energetically disordered system with Gaussian distribution of hopping sites predicting a localization threshold within the tail of the DOS. Upon exciting below ν_{loc}, defect states, identified as precursers of trap II emission, are populated directly as evidenced by the linear shift of the emission energy on ν_{ex}. They are subject to structural relaxation after excitation characterized by an electron–phonon coupling constant $S = 3$. Fluorescence excitation spectra indicate that the excimer-forming site can be excited directly as well as via diffusive and long-range Förster transfer, indicating that excitation of the low-energy pair state is not forbidden.

Acknowledgment. Numerous discussions with R. Richert are gratefully acknowledged as is the financial support by the Deutsche Forschungsgemeinschaft and the Fonds der Chemischen Industrie. We also thank M. Gailberger for synthesizing the copolymer and Professor W. Klöpffer for PVCA samples.

References and Notes

(1) Klöpffer, W. In *Electronic Properties of Polymers*; Mort, J., Pfister, G., Eds.; Wiley: New York, 1982; p 161.
(2) Guillet, J. In *Polymer Photophysics and Photochemistry*; Cambridge University Press: Cambridge, England, 1985; p 241.
(3) Klöpffer, W. In *Photophysics of Polymers*; Hoyle, C. E., Torkelson, J. M., Eds.; ACS Symposium Series 358; American Chemical Society: Washington, DC, 1987; p 264.
(4) Wolf, H. C.; Port, H. *J. Lumin.* **1976**, *12/13*, 33.
(5) Schmid, D. In *Organic Molecular Aggregates*; Reineker, P., Haken, H., Wolf, H. C. Eds.; Springer Serines in Solid State Sciences; Springer Verlag: Berlin, 1983; Vol. 49, p 184.
(6) Masuhara, H.; Tamai, N.; Mataga, N. *Chem. Phys. Lett.* **1982**, *91*, 209.
(7) Peter, G.; Bässler, H.; Schrof, W.; Port, H. *Chem. Phys.* **1985**, *94*, 445.
(8) Bai, F.; Chang, C. H.; Webber, S. E. *Macromolecules* **1986**, *19*, 2484.
(9) Itaya, A.; Sakai, H.; Masuhara, H. *Chem. Phys. Lett.* **1987**, *138*, 231.
(10) Johnson, G. E. *J. Chem. Phys.* **1975**, *62*, 4617.
(11) Itaya, A.; Okamoto, K.; Kusabayashi, S. *Bull. Chem. Soc. Jpn.* **1976**, *49*, 2082.
(12) Rippen, G.; Kaufmann, G.; Klöpffer, W. *Chem. Phys.* **1980**, *52*, 165.
(13) Kenkre, V. M.; Parris, P. E.; Schmid, D. *Phys. Rev. B* **1985**, *32*, 4946.
(14) Bässler, H., *Phys. Status Solidi B* **1981**, *107*, 6.
(15) Eiermann, R.; Parkinson, G. M.; Bässler, H.; Thomas, J. M. *J. Phys. Chem.* **1983**, *87*, 549.
(16) Jankowiak, R.; Rockwitz, K. D., Bässler, H. *J. Phys. Chem.* **1983**, *87*, 552.
(17) Kauffmann, H. F.; Mollay, B.; Weixelbaumer, W. D.; Bürbaumer, J.; Riegler, M.; Meisterhofer, E.; Aussenegg, F. R. *J. Chem. Phys.* **1986**, *85*, 3566.
(18) Personov, R. I. In *Spectroscopy and Excitation Dynamics of Condensed Molecular Systems*; Agranovich, V. M., Hochstrasser, R. M., Eds.; North Holland: Amsterdam, The Netherlands, 1983; p 555.
(19) Elschner, A.; Bässler, H. *Chem. Phys.* **1987**, *112*, 285.
(20) Friedrich, J.; Swalen, J. D.; Haarer, D. *J. Chem.* Phys. **1980**, *73*, 705.
(21) Grünewald, M.; Pohlmann, B.; Movaghar, B.; Würtz, D. *Philos. Mag. B* **1984**, *49*, 341.
(22) Movaghar, B.; Grünewald, M.; Ries, B.; Bässler, H.; Würtz, D. *Phys. Rev. B* **1986**, *33*, 5345.
(23) Movaghar, B.; Ries, B.; Grünewald, M. *Phys. Rev. B* **1986**, *34*, 5574.
(24) Lange, J.; Ries, B.; Bässler, H. *Chem. Phys.* **1988**, *128*, 47.
(25) Richert, R.; Bässler, H.; Ries, B.; Movaghar, B.; Grünewald, M. *Philos. Mag. Lett.* **1989**, *59*, 95.
(26) Schönherr, G.; Bässler, H.; Silver, M. *Philos. Mag. B* **1981**, *44*, 361.
(27) Rughooputh, S. D. D. V.; Bloor, D.; Phillips, D.; Jankowiak, R.; Schütz, L.; Bässler, H. *Chem. Phys.* **1988**, *125*, 355.
(28) Jankowiak, R.; Bässler, H. *Chem. Phys.* **1983**, *79*, 57.
(29) Schneider, F. *Z. Naturforsch.* **1969**, *24A*, 803.
(30) Rockwitz, K. D.; Bässler, H. *Chem. Phys.* **1982**, *70*, 307.
(31) Bogner, U.; Bertes, K.; Schätz, P.; Maier, M. *Chem. Phys. Lett.* **1984**, *110*, 528.
(32) Kador, L.; Schulte, G.; Haarer, H. *J. Chem. Phys.* **1986**, *90*, 1264.
(33) Klöpffer, W.; Bauser, H. *Z. Phys. Chem. (Munich)* **1976**, *101*, 25.
(34) Fitzgibbon, P. D.; Frank, C. F. *Macromolecules* **1982**, *15*, 733.
(35) Cohen, M. D.; Klein, E.; Ludmer, Z.; Yakhot, V. *Chem. Phys.* **1974**, *5*, 15.
(36) Argyrakis, P.; Kopelman, R. *Chem. Phys.* **1980**, *51*, 9.
(37) Klöpffer, W. *Chem. Phys.* **1981**, *57*, 75.
(38) Ries, B.; Bässler, H.; Grünewald, M.; Movaghar, B. *Phys. Rev. B* **1988**, *37*, 5508.
(39) Gösele, U.; Hauser, M.; Klein, U. K. A.; Frey, R. *Chem. Phys. Lett.* **1975**, *34*, 519.
(40) Schrof, W.; Betz, E.; Port, H.; Wolf, H. C. *Chem. Phys.* **1987**, *118*, 57.
(41) Stolzenburg, F.; Ries, B.; Bässler, H. *J. Mol. Electron.* **1987**, *3*, 149.
(42) Klafter, J.; Blumen, A. *Chem. Phys. Lett.* **1985**, *119*, 377.

Registry No. PVCA, 25067-59-8; (styrene)(vinylcarbazole) (copolymer), 26710-15-6.